

## HIGH PURITY ZnS/Ge INTERFERENCE FILTER EMITTANCE

August 1999

Russel E. Clement  
Space and Naval Warfare Systems Center – San Diego  
San Diego, Ca 92152

Clyde Elliott  
U.S. Army Space and Missile Defense Command  
Huntsville, Al 35807

Jon Fisher  
Mission Research Corporation  
Huntsville, Al 35807

### ABSTRACT

Data are presented that demonstrate infrared thin film interference filters made with CVD zinc sulfide start materials exhibit significantly higher spectral emittance than those made with IRTRAN II. A simple radiometric model and comparative analysis are discussed that indicates elevated filter emittance levels may adversely impact infrared sensors and seekers designed to operate in the 7 - 15 micron region. It is expected that systems that incorporate filters made with CVD ZnS could exhibit anomalous high backgrounds, image blurring or optical cross talk.

### 1.0 Introduction

Thin film interference filters are incorporated in infrared sensor and seeker designs for ballistic missile defense (BMD) applications providing wavelength definition and separation while operating at cryogenic temperatures. In most cases the filter immediately precedes the focal plane array in the optical train of the system, thus setting the critical background photon flux on the imaging element. The optical properties of these filters have a significant impact on the performance of the infrared sensor/seeker system and therefore require very exacting tolerances for in-band and out-of-band transmittance ( $T^*$ ) as well as emittance ( $\epsilon$ ) over the wavelength sensitivity region of the system's focal plane array.

Numerous demonstration programs and experiments funded by the DoD over the last 10 - 15 years have been utilized for testing the performance of filter and focal plane combinations for ballistic missile defense. As a result of these efforts, certain long-standing transmittance requirements for filters have been validated. Multi-color IR sensors that include filter pass-bands in the 7 - 15 micron region provide useful tracking and discrimination options however require very effective blocking ( $T^* < 10^{-4}$ ) in the short wavelength region and steep band-edge slopes for BMD missions. Interference filters made of

| REPORT DOCUMENTATION PAGE  |             |                                      |                               | Form Approved<br>OMB No. 0704-01-0188       |   |  |
|--|-------------|--------------------------------------|-------------------------------|---|---|--|
| The public reporting burden for this collection of information is estimated to average 1 hour per response, including the time for reviewing instructions, searching existing data sources, gathering and maintaining the data needed, and completing and reviewing the collection of information. Send comments regarding this burden estimate or any other aspect of this collection of information, including suggestions for reducing the burden to Department of Defense, Washington Headquarters Services, Directorate for Information Operations and Reports (0704-0188), 1215 Jefferson Davis Highway, Suite 1204, Arlington VA 22202-4302. Respondents should be aware that notwithstanding any other provision of law, no person shall be subject to any penalty for failing to comply with a collection of information if it does not display a currently valid OMB control number. |             |                                      |                               |   |   |  |
| PLEASE DO NOT RETURN YOUR FORM TO THE ABOVE ADDRESS.   |             |                                      |                               |   |   |  |
| 1. REPORT DATE (DD-MM-YYYY)<br><del>01-10-1999</del>   |             | 2. REPORT TYPE<br>Professional Paper |                               | 3. DATES COVERED (From - To)                |   |  |
| 4. TITLE AND SUBTITLE<br><br>High Purity ZnS/Ge Interference Filter Emittance  |             |                                      |                               | 5a. CONTRACT NUMBER                         |   |  |
|  |             |                                      |                               | 5b. GRANT NUMBER                            |   |  |
|  |             |                                      |                               | 5c. PROGRAM ELEMENT NUMBER<br>0407700D      |   |  |
|  |             |                                      |                               | 5d. PROJECT NUMBER<br>XA02                  |   |  |
| 6. AUTHORS<br><br>Clement, Russel E.<br>Elliott, Clyde<br>Fisher, Jon  |             |                                      |                               | 5e. TASK NUMBER                             |   |  |
|  |             |                                      |                               | 5f. WORK UNIT NUMBER                        |   |  |
|  |             |                                      |                               |   |   |  |
| 7. PERFORMING ORGANIZATION NAME(S) AND ADDRESS(ES)<br>Space and Naval Warfare Systems Center<br>53560 Hull Street<br>San Diego, CA 92152-5001  |             |                                      |                               | 8. PERFORMING ORGANIZATION<br>REPORT NUMBER |   |  |
| 9. SPONSORING/MONITORING AGENCY NAME(S) AND ADDRESS(ES)<br>U.S. Army Strategic Defense Command<br>CSSD-BM-EAC<br>P.O. Box 1500<br>Huntsville, AL 35807-3801  |             |                                      |                               | 10. SPONSOR/MONITOR'S ACRONYM(S)            |   |  |
|  |             |                                      |                               | 11. SPONSOR/MONITOR'S REPORT<br>NUMBER(S)   |   |  |
|  |             |                                      |                               |   |   |  |
| 12. DISTRIBUTION/AVAILABILITY STATEMENT<br>Approved for public release; distribution is unlimited.   |             |                                      |                               |   |   |  |
| 13. SUPPLEMENTARY NOTES  |             |                                      |                               |   |   |  |
| 14. ABSTRACT<br><br>Data are presented that demonstrate infrared thin film interference filters made with CVD zinc sulfide start materials exhibit significantly higher spectral emittance than those made with IRTRAN II. A simple radiometric model and comparative analysis are discussed that indicates elevated filter emittance levels may adversely impact infrared sensors and seekers designed to operate in the 7 - 15 micron region. It is expected that systems that incorporate filters made with CVD ZnS could exhibit anomalous high backgrounds, image blurring or optical cross talk.<br><br><br>Published in Proceedings of 1999 Meeting of the MSS Specialty Group on Infrared Materials, Vol. 1, Issue No. 1, pp. 129-141, October 1999.   |             |                                      |                               |   |   |  |
| 15. SUBJECT TERMS<br>Command, Control, and Communications<br>sensors      infrared      electro-optics<br>radiometry   detectors   devices   |             |                                      |                               |   |   |  |
| 16. SECURITY CLASSIFICATION OF:  |             |                                      | 17. LIMITATION OF<br>ABSTRACT |   | 18. NUMBER<br>OF<br>PAGES                                   |  |
| a. REPORT  | b. ABSTRACT | c. THIS PAGE                         |                               |   | 19a. NAME OF RESPONSIBLE PERSON<br>Wernli, Robert L.        |  |
| U  | U           | U                                    |                               |   | 19b. TELEPHONE NUMBER (Include area code)<br>(619) 553-1948 |  |

alternating layers of zinc sulfide and germanium (ZnS/Ge) are most commonly used for pass-bands in the 7 - 15 micron region where few high-low refractive index material combinations are available. ZnS/Ge filter technology is in fact the only material combination that has been shown to meet the most exacting out-of-band and in-band transmittance as well as band-edge requirements of state-of-the-art infrared systems.

In recent years, the primary manufacturers of the ZnS/Ge filter technology have switched from IRTRAN II to chemical vapor deposited (CVD) zinc sulfide as a start material in the filter layer deposition process. There is evidence that concurrent with this change, the spectral emittance and out-gas times of new ZnS/Ge filters have increased substantially from that of the filter technology employed in prior infrared sensor/seeker validation efforts. Filters made with CVD ZnS exhibit 2 to 10 times higher spectral emittance than those made with IRTRAN II with the greatest relative spectral emittance increases seen in the in-band wavelengths. This study is an effort to quantify those changes in filter performance as well as project the potential impact on infrared sensors and seeker systems currently under development.

## 2.0 Background

During the late 1970s and early 1980s, out-of-band spectral characteristics of filters were extremely susceptible to the presence of absorption and scatter centers (Stierwalt, 1974) which established the lower limit to the out-of-band transmittance of these components. Significant efforts were funded at that time by the DoD and other government agencies to improve the radiometric performance of thin film interference filters through optimization of material properties and film deposition techniques. For pass-bands in the 7 - 15 micron region, ZnS/Ge made from IRTRAN II became the dominant thin film filter technology meeting the most stringent out-of-band ( $T^* < 10^{-5}$ ) and band-edge ( $m < 1\%$ ) performance requirements while minimizing what has since become known as the Stierwalt effect.

During the late 1980s, a series of experiments under sponsorship of the U.S. Army Space and Strategic Defense Command (now called USASMD) were conducted at the Naval Ocean Systems Center (now called SSC-SD) to test the performance of thin film interference filter technologies in high dose gamma radiation environments. Tests conducted on filters of various pass-band and material designs at cryogenic temperatures indicated that structures made with some IRTRAN variants were susceptible to transmittance degradation at total dose levels below 10 kilorads (Clement and Stierwalt, 1991). Immediately, filter-hardening efforts began to focus on making ZnS/Ge filters using CVD ZnS as a start material in the hopes that IRTRAN II impurities were the cause of the radiation degradation.

The first filters made with CVD ZnS exhibited much less gamma induced transmittance degradation than the earlier ones made with IRTRAN II, however, some of the data at the time indicated that substituting CVD ZnS caused the out-of-band radiometric performance to degrade from the levels established by the older filter technology. There was some thought in the infrared radiometry and radiation hardening communities that perhaps programs were overstating the out-of-band transmittance requirements on the filter technology at the time and new filters made with CVD ZnS were in fact adequate for ballistic missile defense requirements. Subsequently, evidence from various targeting and tracking demonstration projects began to indicate this was not the case and that the original filter radiometric filter requirements may be necessary for infrared sensor and seeker systems to adequately perform their function within the BMD system architecture.

Since the primary manufacturers of ZnS/Ge interference filter technology had switched to using CVD ZnS as a start material, it was necessary to address the radiometric issue in the filter designs themselves by increasing the out-of-band blocking at the expense of some in-band transmittance. ZnS/Ge filters developed for recent NASA and DoD programs and made with CVD ZnS have been able to meet out-of-band transmission requirements in the  $10^{-5}$  range while maintaining in-band transmittance above

70%. Radiometric testing of these filters at operational temperatures however detected a significant increase in the spectral emittance compared to pre-CVD ZnS filter technology traceable to the substitution of CVD ZnS for IRTRAN II. The emittance ( $\epsilon$ ) levels observed in these samples is well above the standard BMD program specification average ( $\sim 0.5\%$ ) over the 1-15 micron region and is accompanied by much higher levels of out-gassing ( $d\epsilon/dt$  under vacuum). It is clear from these recent results that ZnS/Ge filters made with CVD ZnS currently may not meet all radiometric performance specifications typically required for ballistic missile defense programs. It is also clear there are no alternative materials or technologies for ZnS/Ge interference filters in the 7 - 15 micron wavelength region that have been demonstrated (either at this facility or in published results) to meet these same radiometric requirements.

Much as with the out-of-band transmittance performance mentioned earlier, there are serious questions as to whether filter emittance specifications may be overly restrictive. There are no unambiguous data available as to the impact the elevated emittance and excessive out-gassing of these filters may have on an operational sensor or seeker. Since CVD ZnS went into general use in making these components only recently, there have been few systems to incorporate them and several that did were cancelled for either financial or undisclosed technical reasons. In those programs that may have run into technical difficulties related to the sensor performance, excess emittance, out-gassing, absorption and scatter in the filter may not have been considered as possible failure mechanisms. Since infrared sensors and seekers employ thin film filters in very different geometric orientations with respect to the focal plane array, the impact of the filter radiometric performance may be very sensor design-specific. To address these issues, an analysis is presented on actual CVD ZnS filter data in generic sensor conditions.

### 3.0 Technical Approach

In this work we extend previous radiometric performance analysis on thin film interference filters made with CVD zinc sulfide. Since complete characterization of the infrared optical properties of a single filter is a time consuming and labor intensive process, investigating a large number of filter samples is cost prohibitive. Instead, a comparative study of two samples believed to be representative of filters made with IRTRAN II fabricated before 1988 and state-of-the-art CVD ZnS technology fabricated in 1997 is presented. Both filters were designed to meet in-band and out-of-band transmittance performance requirements consistent with current infrared sensor and seeker programs in the 7 - 15 micron pass-band region.

The approach to this experiment was to measure the radiometric characteristics of one filter made with IRTRAN II and another made more recently with CVD ZnS with similar pass bands and out-of-band transmission levels. These measurements were conducted at temperatures and geometry representative of current state-of-the-art sensor and seeker system designs for ballistic missile defense applications. To assess the radiometric effects of filter emittance on sensor internal photonic environment, a simple analytical model was developed for isothermal enclosures. It is believed the simplifying assumptions included in this model provide for a conservative estimate of sensor performance parameters established by using CVD ZnS filter technology.

### 4.0 Theory

Infrared energy incident on the surface of an interference filter at thermal equilibrium must be absorbed, transmitted or reflected in accordance with the relationship

$$A_{\lambda} + R_{\lambda} + T_{\lambda} = 1 \quad (1)$$

where

$A_\lambda$  = fraction of energy absorbed,  
 $R_\lambda$  = fraction of energy reflected,

and

$T_\lambda$  = fraction of energy transmitted.

For partially transparent samples with parallel, nearly specular surfaces, McMahon (1950) derived the following relationships:

$$A^*_\lambda = \epsilon_\lambda = (1-r^2)(1-e^{-\alpha d})/(1-r^2e^{-\alpha d}), \quad (2)$$

$$R^*_\lambda = r^2[1+e^{-2\alpha d}-2r^2]/(1-r^4e^{-2\alpha d}) \quad (3)$$

and

$$T^*_\lambda = (1-r^2)^2e^{-\alpha d}/(1-r^4e^{-2\alpha d}) \quad (4)$$

where

$\epsilon_\lambda$  = ratio of thermal radiation emitted per unit area to that of a blackbody at the same temperature,

$r = (n-1)/(n+1)$ ,

$n$  = real part of the complex refractive index,

$\alpha$  = absorption coefficient

and  $d$  is the sample thickness.

It can be shown from equations (2-4) that

$$1 = T^*_\lambda + R^*_\lambda + \epsilon_\lambda. \quad (5)$$

## 5.0 Test Method

Instruments to measure the transmittance ( $T^*$ ) and emittance ( $\epsilon$ ) of cryogenically cooled samples in the 1.5 - 50 micron region have been developed at SSC-SD with previously published test methodologies and operational details based on the Beckman IR-3 spectrophotometer (Stierwalt et al., 1963). The IR-3 is a single beam instrument having two monochromators ganged together with a central aperture. The fully evacuated, compartmented design of the IR-3 maintains high spectral purity by attenuating scattered energy to less than one part in one million. Thermal stability of the IR-3 is maintained through use of a water bath. Potassium bromide prisms are employed in the current setup to achieve the maximum wavelength resolution in the 1.5 - 25 micron region. The built-in reference detector used in this investigation was a Beckman model 10360 thermocouple with a cesium iodide window. The energy response of the thermocouple was monitored with a built-in transformer and pre-amp connected to an EG&G Princeton Applied Research model 5210 lock-in amplifier. Data were collected from the lock-in over a GPIB bus by a microcomputer. The microcomputer was used to also control the UNIDEX-11 model U11R 4-axis controller for setting the wavelength and slit width of the spectrophotometer using stepper motors.

Transmittance data presented in this report were developed as in/out measurements at an approximate 6-inch working distance (spectrometer mode). The spectrophotometer test Dewar was vacuum interfaced to the gas cell chamber of the IR-3 spectrophotometer with the tailpiece of the test Dewar extending directly into the exit beam path of the instrument. Masking the sample to the appropriate size controlled the cone shape of the incident radiation.

Emissance data were collected using a second IR-3 system with the test sample mounted in a cryostat vacuum interfaced to the source compartment. In this configuration, the cryo-cooled sample acts as the signal source of the monochromator system. The infrared emission from the sample was chopped against a blackbody maintained at 25°C. The a-c signal recorded for the sample body was then compared to that of a calibrated black cavity substituted in the sample holder and maintained at the same temperature as the filter under test. The spectral properties of the black cavity can be seen in Figure 1.

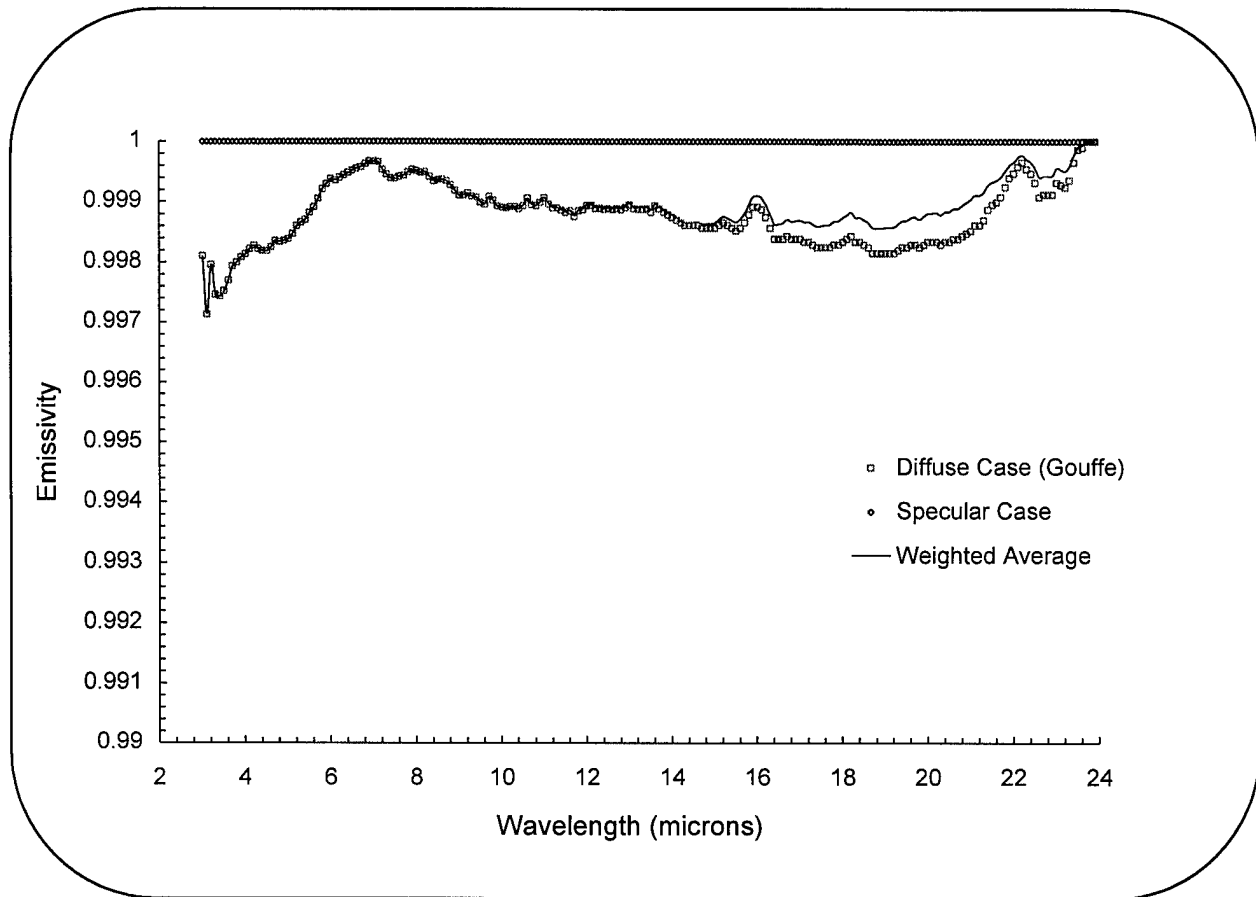


Figure 1. Modeled Black Cavity Performance.

Two techniques were employed for measurement of the filter emittance properties. The first technique was to place the black cavity in the sample holder behind the partially transparent filter. In this orientation, the black cavity is at the same temperature as the filter under test thus optimizing the signal-to-noise ratio for assessing materials with very low absorption properties. Stierwalt et al. (1963) developed a model for the operation of the IR-3 with a fundamental energy equation in this test mode

$$S_s = K(\epsilon W_s + R^* W_m + T^* W_s - W_m) \quad (6)$$

where

$S_s$  = measured thermocouple signal with test sample in place,  
 $W_m$  = emission of a blackbody at the temperature of the monochromator,

and

$W_s$  = emission of a blackbody at the sample temperature.

The ratio of the energy detected from the sample under test ( $S_s$ ) to a reference black cavity ( $S_{bc}$ ,  $\epsilon_{bc} \sim 1$ ) can then be used to determine the sum of the transmittance and emittance from

$$T^* + \epsilon = S_s / S_{bc} (W_{bc} - W_m) / (W_s - W_m) \quad (7)$$

$S_{bc}$  = measured thermocouple signal with only the black cavity in place,  
 $W_{bc}$  = emission of a blackbody at the temperature of the black cavity.

When the black cavity and the sample are at the same temperature,  $W_s$  is equal to  $W_{bc}$  and

$$T^* + \epsilon = S_s / S_{bc}. \quad (8)$$

From measured transmittance ( $T^*$ ) results related in temperature, wavelength and solid angle, the emittance of the test sample was then determined from equation (8).

The second technique for measurement of the filter emittance was to remove the black cavity from behind the filter sample during measurement. In this measurement mode, Stierwalt's fundamental energy equation takes the form

$$S_s = K(\epsilon W_s + R^* W_m + T^* W_m - W_m). \quad (9)$$

In this test mode ( $\epsilon$ -mode), the ratio of the measured sample energy ( $S_s$ ) to that of the black cavity ( $S_{bc}$ ) is a direct measurement of the sample emittance

$$S_s / S_{bc} = \epsilon. \quad (10)$$

The second method is useful for materials that exhibit significant amounts of absorption and has the advantage of requiring only a single measurement at a given temperature while not relying on a focussed transmittance measurement. As such, this method is less sensitive to optical scatter-related complications (Hanssen and Kaplan, 1998) in the emittance measurements. Comparison of the test results using both measurement techniques is a unique tool for detecting the presence of optical scatter in partially transparent samples.

## 6.0 Results

Figures 2 and 3 are emittance spectra of the CVD ZnS/Ge filter and the older IRTRAN II ZnS/Ge filter at 85 Kelvin using the  $T+\epsilon$  mode of emittance testing. (Included in Figure 3 is a plot of the emittance characteristics of a typical gold mirror coating for test system out-gas characteristic reference.) The sample made from CVD ZnS start materials exhibited emittance characteristics averaging more than

10% over the entire spectral region even after prolonged out-gas periods. The measured emittance of the filter made with IRTRAN II was less than half that of the new state-of-the-art sample. Both samples required in excess of 17 hours under vacuum to reach minimum emittance levels. The CVD ZnS/Ge required substantially longer than the older sample to reach its minimum level. The time dependent emittance data were collected at approximate 24-hour intervals following the initial 17-hour period. The minimum emittance results in Figures 2 and 3 represent the earliest observation when each filter's optimal performance was recorded.

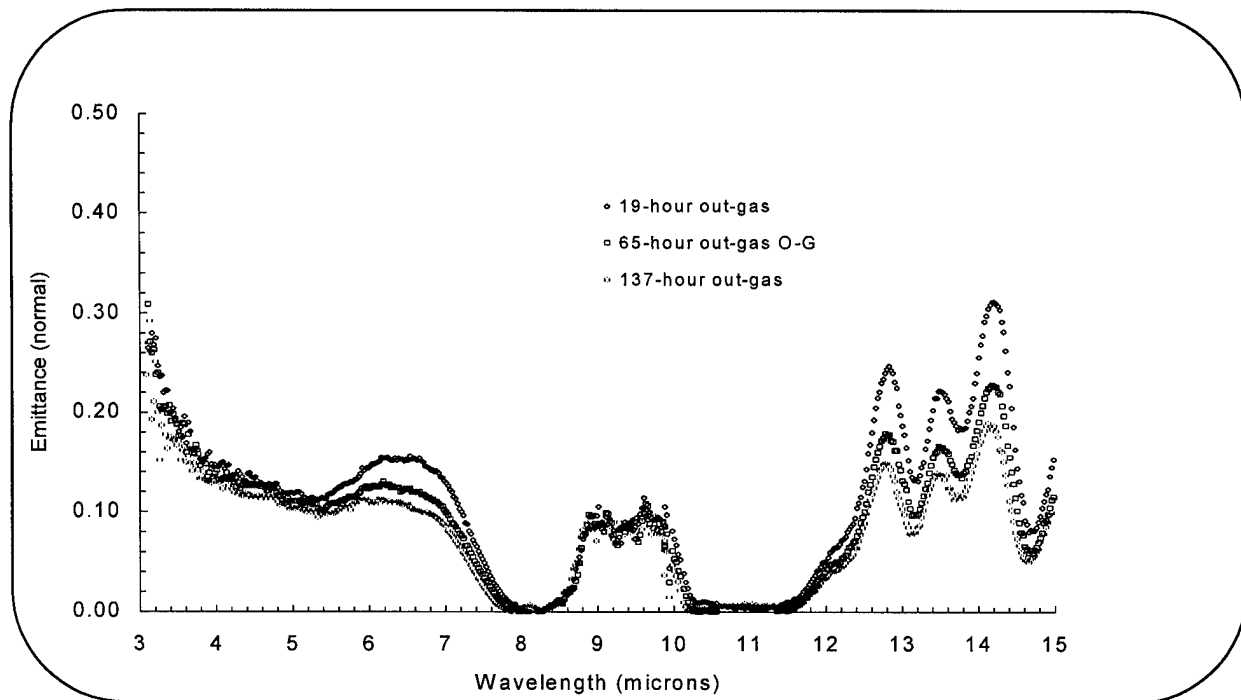


Figure 2. CVD ZnS/Ge MWIR Filter ( $T = 85$  K).

Emission features in the 5 - 8 micron region and 12-15 micron region for both filters resemble atmospheric components of water vapor and carbon dioxide. Since neither of these emission features are strongly apparent in the measurements of the gold coating (see Fig. 3), it is concluded that these constituents are absorbed in the filters themselves. These two components make up the majority of the time dependent out-gas variations. The in-band emittance from the filter in Figure 2 (8.5 - 10 microns) was not out-gas time dependent and is representative of features consistently observed throughout the pass-bands of filters made with CVD ZnS. Although it is not clear what could be causing this emittance feature, follow-up testing in the  $\epsilon$ -mode emittance technique (discussed earlier) is approximately 50% of the  $T^* + \epsilon$  mode results (see Fig. 4). The test-mode-dependent results may be explained by the presence of photonic scatter originating in the filter.

## 7.0 Analysis

In infrared sensor configurations incorporating thin film interference filters, the sensor photon background incident on the focal plane is largely set by the optical properties of the thin film filter (including transmission, reflection and emission properties). In order to discuss the relative significance of each of these three filter performance parameters, it is necessary at this point to introduce a simplified radiometric analysis for a generic component arrangement in an idealized infrared sensor chamber.



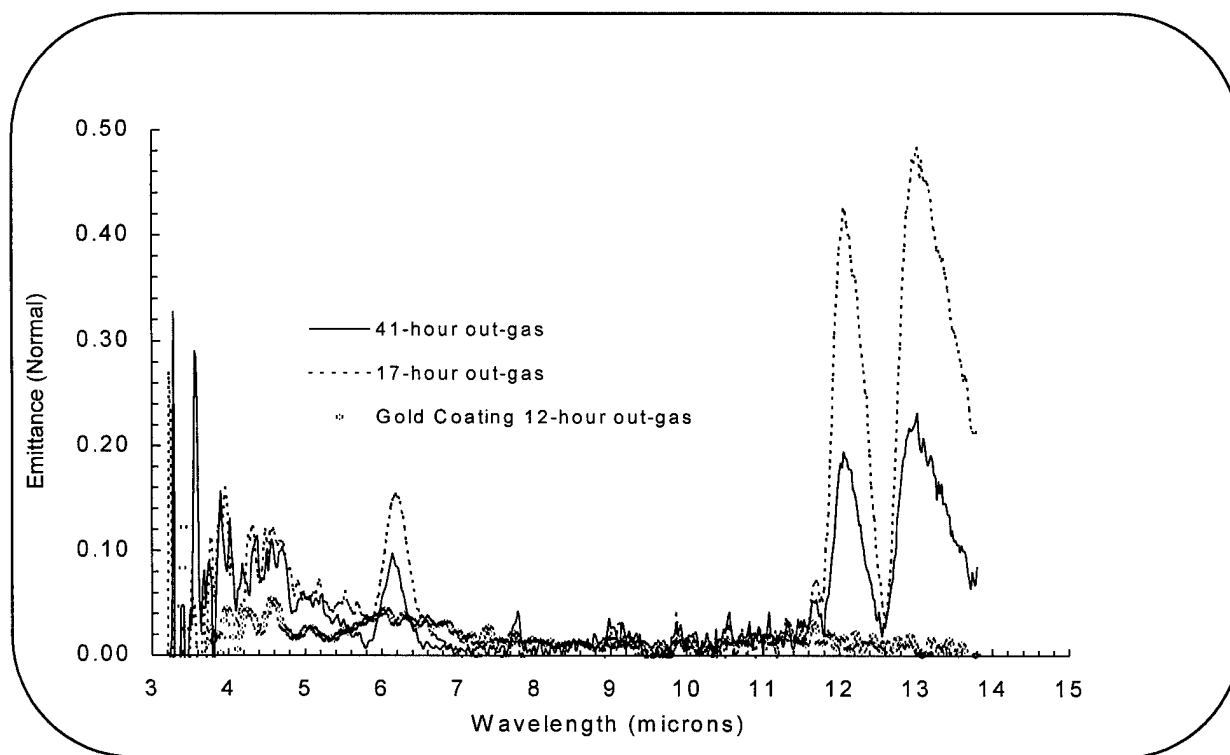


Figure 3. IRTRAN II ZnS/Ge MWIR Filter ( $T = 85$  K).

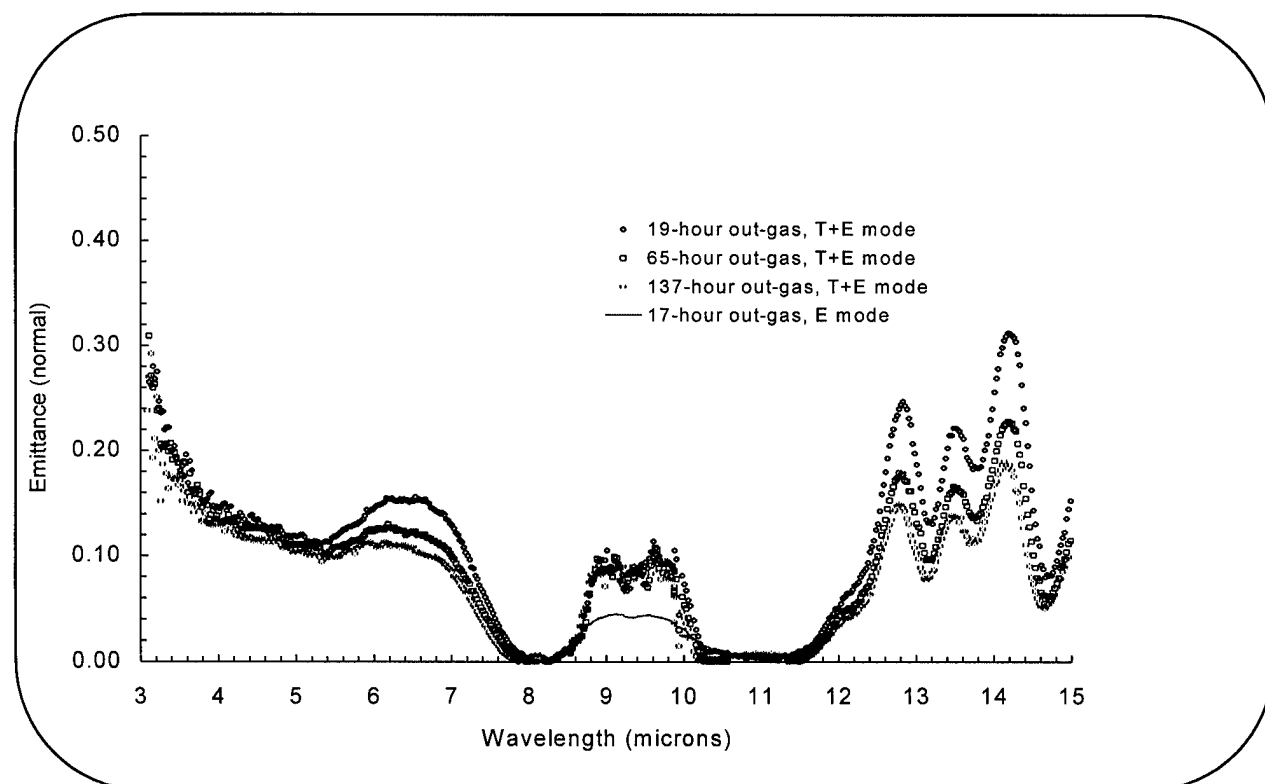


Figure 4. CVD ZnS/Ge MWIR Filter Test Mode Comparison ( $T = 85$  K).

Figure 5 is a diagram of an enclosure that represents the sensor heat shield surrounding a filter and focal plane. Three points in and on the enclosure are identified as a function of temperature ( $T_n$ ). For the sake of this discussion, it is assumed that  $T_1=T_2=T_3$  is sufficient for isothermal conditions to exist. The isotropic photon flux distribution at point P ( $F_\lambda(P)$ ) generated by the enclosure and its contents is

$$F_\lambda(P) = \oint I_\lambda \cos\theta \, d\omega \quad (11)$$

where the specific intensity ( $I_\lambda$ ) is the radiant energy ( $\text{cm}^{-2} \text{sec}^{-1}$ ) of wavelength  $\lambda$  in the direction of angle  $\theta$  and  $\phi$  ( $\text{ster}^{-1}$ ). For a blackbody,

$$I_\lambda = B_\lambda = 2hc^2/(\lambda^5(e^{hc/\lambda kt} - 1)) \text{ erg cm}^{-2} \text{ sec}^{-1} \text{ cm}^{-1} \text{ ster}^{-1}. \quad (12)$$

The flux at point P can then be represented as

$$F_\lambda(P) = \oint I_{\lambda \text{encl}} \cos\theta d\omega + \oint I_{\lambda \text{fil}} \cos\theta d\omega. \quad (13)$$

Substituting  $d\omega = \sin\theta d\theta d\phi$ ,

$$F_\lambda(P) = \int_0^{2\pi} \int_0^{\pi/2} I_{\lambda \text{encl}} \cos\theta \sin\theta d\theta d\phi + \int_0^{2\pi} \int_0^{\theta} I_{\lambda \text{fil}} \cos\theta \sin\theta d\theta d\phi \quad (14)$$

which may be calculated as

$$F_\lambda(P) = \pi I_{\lambda \text{encl}}(1 - \sin^2\theta) + \pi I_{\lambda \text{fil}} \sin^2\theta. \quad (15)$$

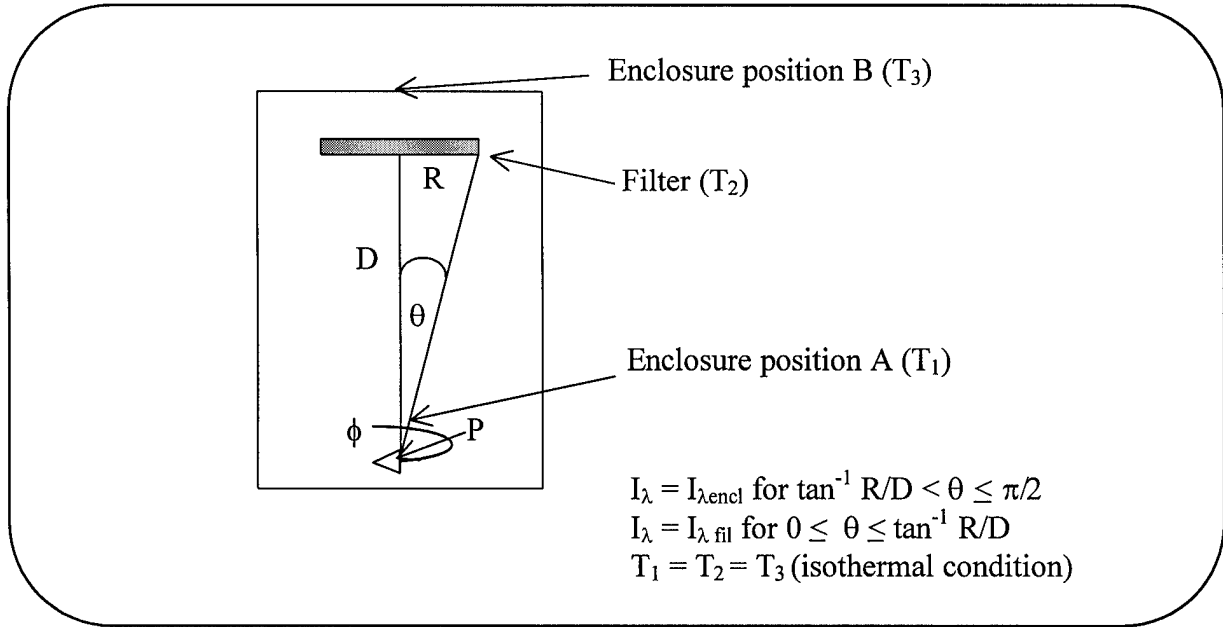


Figure 5. Schematic of isothermal enclosure.

In the most general case for the configuration in Figure 5, the photon flux at point P on the focal plane is

$$F_{\lambda}(P) = \pi(\epsilon_{\lambda\text{encl}} + R_{\lambda\text{encl}}^*)B_{\lambda}(T_1)(1 - \sin^2\theta) + \pi(\epsilon_{\lambda\text{fil}}B_{\lambda}(T_2) + R_{\lambda\text{fil}}^*B_{\lambda}(T_1) + T_{\lambda\text{fil}}^*(\epsilon_{\lambda\text{encl}} + R_{\lambda\text{encl}}^*)B_{\lambda}(T_3)) \sin^2\theta. \quad (16)$$

From this equation it is clear that under isothermal conditions ( $T_1=T_2=T_3$ ), the emittance of the filter ( $\epsilon_{\lambda\text{fil}}$ ) is of minimal significance to the total photon flux at point P because any emittance variance is offset by a co-variance in the filter reflectance and/or transmittance. On the other hand, it is common in IR sensors for the filter temperature to be greater than the focal plane temperature ( $T_2>T_1$ ), therefore  $B_{\lambda}(T_2)>B_{\lambda}(T_1)$ . When this occurs, the contribution from filter emittance becomes more significant because emitted filter flux variances are not directly offset by the terms containing the reflectance and transmittance parameters. Photon flux contribution from the filter itself may therefore be a significant consideration in infrared sensor chambers that are not isothermal enclosures.

It is beyond the scope of this paper to address actual sensor operational scenarios using this simple model. However, it is useful to use the filter emittance term from equation (16) to determine the range of internal photon background contributions that may be expected from a real filter over a range of reasonable temperatures and geometry. The filter-emitted photon flux for an isotropic energy distribution at point P is

$$F_{\lambda}(P) = \epsilon_{\lambda\text{fil}}(B_{\lambda}(T_2))\pi\sin^2\theta. \quad (17)$$

From Figure 5,

$$\sin\theta = R/(R^2+D^2)^{1/2}, \quad (18)$$

which can be rewritten in terms of the solid angle the filter subtends of the detector field-of-view or filter f-number ( $f\# = D/2R$ ) such that

$$F_{\lambda}(P) = \epsilon_{\lambda}B_{\lambda}\pi/(1+4[f\#]^2). \quad (19)$$

Figure 6 is a plot of the filter-generated photon flux for a filter at 85 Kelvins using emittance characteristics from the data in Figures 2 and 3 as a function of filter f-number ( $f\#$ ). (Note: this is not sensor system f-number.) As the filter  $f\#$  goes to 0 (focal plane mode), the filter-generated integrated background flux in the 3 - 14 micron region is determined to be  $5.9061 \times 10^{12}$  photons/cm<sup>2</sup>/sec using the 186 hour out-gas emittance ( $\epsilon_{\lambda}$ ) data for the DoD filter constructed from CVD ZnS. The results for the filter constructed from IRTRAN II (41 hour out-gas) in the focal plane mode limit was determined to be  $3.6087 \times 10^{12}$  photons/cm<sup>2</sup>/sec. The emittance differential between the two filter samples represents a minimum 63.7% increase for the CVD technology in filter-generated photon background flux in all calculated  $f\#$  configurations at this temperature.

Follow-up tests on the filter made with CVD ZnS indicated the spectral emittance ( $\epsilon$ ) was nearly constant in the 3 - 12.5 micron region over temperatures ranging from 75 - 115 Kelvins. Figure 7 is a plot of the modeled filter-generated photon backgrounds from the 137 hour out-gas data in Figure 4 over this temperature range. The modeled photon backgrounds at the higher temperatures are comparable to total sensor background limits expected in most BMD sensor/seeker programs.

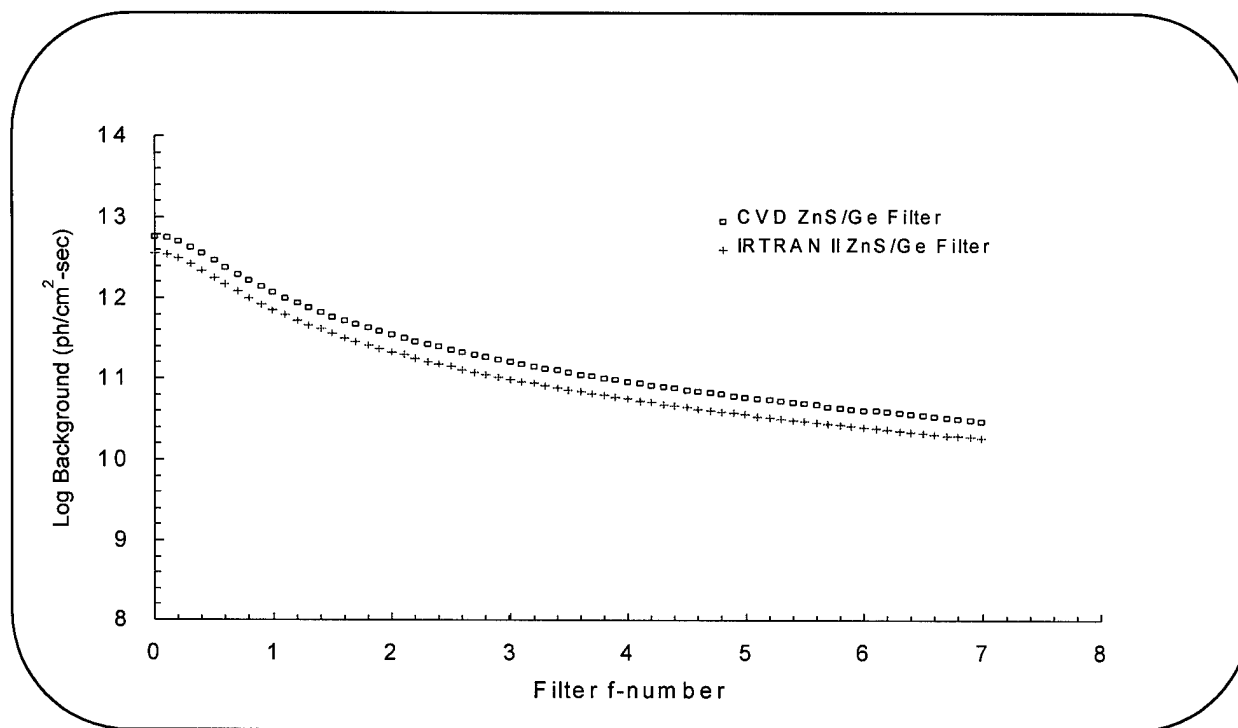


Figure 6. Filter-generated Background Photon Flux Model Estimate ( $T = 85$  K, 3-14 microns).

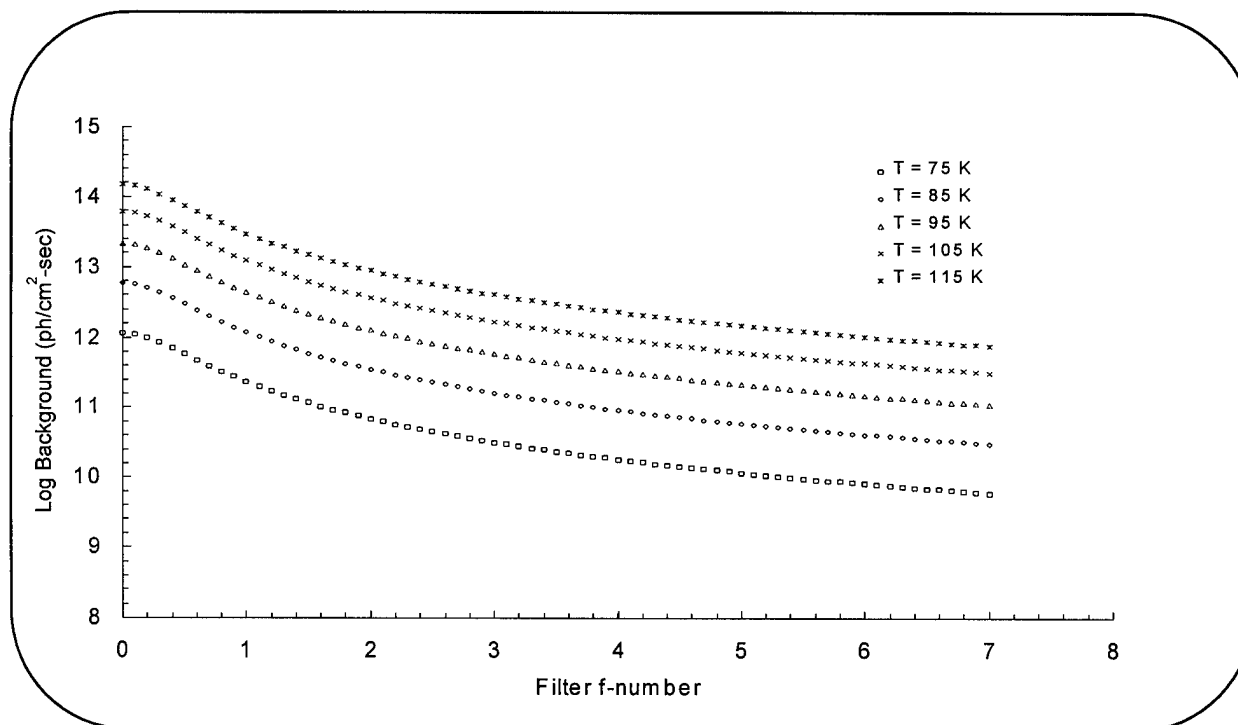


Figure 7. CVD ZnS/Ge Filter-generated Background Photon Flux Model Estimate.

## 8.0 Discussion

The filter-generated photon background is just one component of the sensor photon environment that is related to the filter optical properties. The total background flux on the focal plane array also depends on the photon flux transmitted through the pass-band of the filter as well as that reflected from the filter. The amount and significance of background flux transmitted or reflected from the filter is strongly dependent on the radiometric characteristics of the infrared sensor and its components. If a particular sensor focal plane enclosure may be modeled as an idealized isothermal chamber, the importance of the relative amount of reflected to emitted filter flux may be lessened. However, since few sensor chambers are truly isothermal, the filter-generated photon flux establishes a lower limit to the achievable background on the sensor focal plane array. This issue is most significant in optically fast sensor configurations in which the filters operate at temperatures greater than 77 Kelvin. It should be noted that the assumption of isotropic energy distribution emanating from the filter surface in deriving the background photon flux as a function of  $f\#$  is likely most valid for near-normal incidence. It is also important to note that since sensor scene background is primarily regulated by the filter, excessive absorption of filters made with CVD ZnS will cause an increase in thermal load on sensor cryogenic systems.

Another problem arising from optical characteristics seen in Figure 2 is related to both the structure and magnitude of the filter emittance characteristics. Some infrared sensors incorporate multiple filters with overlapping pass-bands in the optical beam to sort spectral properties of both the intended signal source and the medium through which the signal source is observed. For staring systems with a large number of narrow pass filters with overlapping pass-bands, a significant portion of the energy transmitted to the secondary filter (located immediately in front of the focal plane) could be energy originating from the preceding filter and not from the intended signal source. When sorting IR signal through the atmospheric absorption bands, the excess energy detected could be interpreted as an erroneously high source signature or possibly an energy leak in the primary sorting filter out-of-band. Since there are an enormously high number of variations in infrared sensor/seeker optical system designs available, the quantitative aspects of this issue are strongly sensor design-specific.

Finally, the filter made using CVD ZnS not only has a higher emittance coefficient than its counterpart in this study, it takes significantly longer to out-gas to its minimum emittance levels in the  $H_2O$  and  $CO_2$  absorption regions than the sample made with IRTRAN II. Filter out-gassing ( $d\epsilon/dt$  under vacuum) may cause a temporal variance in the optical properties of systems that are rapidly pumped out and cooled. The in-band emittance of the filter made with CVD ZnS does not show the out-gas-time dependence possibly indicating a different mechanism than the out-of-band absorption. An effort is currently underway at SSC-SD to investigate the nature of the in-band absorption. The test-mode-dependent differential in emittance results is consistent with the presence of photonic scatter. Photonic scatter effects that originate in the filter element located in front of a focal plane array could cause image blurring due to optical cross-talk. This effect could also be interpreted as elevated backgrounds in multi-target scene simulations or as a larger than expected diffraction limit of an IR seeker or sensor.

## 9.0 Summary

The data presented in this report indicate current state-of-the-art long wave infrared thin film interference filters fabricated using CVD ZnS can exhibit significantly higher spectral emittance than filters fabricated with IRTRAN II. The degradation in filter emittance performance is significant to the extent that current filters can not meet a typical program specification of  $\langle \epsilon \rangle \leq 5\%$ . The elevated emittance characteristics of current state-of-the-art interference filters can have a potentially significant impact on the photon background and issues concerning radiometry of new BMDO sensors and seeker systems.

## REFERENCES

- Clement, R.E. and Stierwalt, D.L. 1991, in Proceedings of the IRIS Specialty Group on Infrared Materials, pg. 111.
- Gouffe, A. 1945, Rev. Optq., 24, 1.
- Hanssen, L. and Kaplan, S. 1998, SPIE Conference Proceedings on Optical Diagnostic Methods for Inorganic Transmissive Materials, 3425, 28.
- McMahon, H.O. 1950, J. Opt. Soc. Am., 40, 376.
- Stierwalt, D.L. et al. 1963, App. Opt., 2, 1169.
- Stierwalt, D.L. 1974, Opt. Eng., 13, 3, G115.